Lineage-based scaling of germline intercellular bridges during oogenesis

Umayr Shaikh[1], Kathleen Sherlock[1], Julia Wilson[1], William Gilliland[2], and Lindsay Lewellyn[1]

[1]Department of Biological Sciences, Butler University
Indianapolis, IN
[2]Department of Biological Sciences, DePaul University
Chicago, IL

Abstract

The size of subcellular structures must be tightly controlled to maintain normal cell function; this is especially important when cells are part of developing tissues or organs. Despite its importance, few studies have determined how the size of organelles or other structures is maintained during tissue growth, when cells are growing, dividing, and rearranging. The developing egg chamber is a powerful model in which to study the relative growth rates of subcellular structures. The egg chamber contains a cluster of sixteen germ cells, which are connected through intercellular bridges called ring canals. Ring canals are formed following incomplete cytokinesis after each of four germ cell divisions. As the egg chamber grows, the nurse cells and the ring canals that connect them increase in size. Here, we demonstrate that ring canal size scaling is related to their lineage; the largest, “first born” ring canals grow at a relatively slower rate than ring canals derived from subsequent mitotic divisions. This lineage-based scaling relationship is maintained even if directed transport is reduced, ring canal size is altered, or if the germ cells go through an additional mitotic division. Further, we propose that changes in ring canal scaling could provide a mechanism to alter egg size.

Introduction

A fundamental question in biology is how size is regulated. There is an extensive literature describing the relationship between body size and the size of organs or appendages (Gayon, 2000; Huxley and Teissier, 1936), but we are just beginning to understand how size is regulated at the cellular level. Cells vary in size from one organism to another and from one cell type to another, but an essential feature of all cells is that they must regulate the size and number of their subcellular structures. Many studies have described the scaling of various organelles with cell size, including the nucleus, the mitotic spindle, mitochondria, the ER, and others (Marshall, 2020), but very little is known about how subcellular scaling is established and maintained within developing tissues, where cells are growing, dividing, and rearranging.

The developing fruit fly egg chamber is a powerful model system to study scaling of subcellular structures. The egg chamber is the functional unit of oogenesis which will ultimately produce the mature egg; within the egg chamber, the developing oocyte and its supporting nurse cells are surrounded by a layer of epithelial cells. The oocyte is connected to the nurse cells through intercellular bridges, called ring canals, which provide a channel for the delivery of essential materials from the nurse cells to the oocyte. From stage 2-14, the egg chamber increases in volume by approximately 1,000-fold (Fig. 1A; Ali-Murthy et al., 2021); therefore, the egg chamber provides us with the opportunity to learn how the size of subcellular structures is coordinated during tissue growth.

One of the most well-established examples of subcellular scaling is that of the nucleus. Cells typically maintain a constant ratio of nuclear to cytoplasmic volume, which appears to be actively maintained in healthy cells. When cells divide, or if cell size is artificially manipulated, the nucleus will adjust its size to re-establish the proper ratio (Balachandra et al., 2022; Cantwell and Nurse, 2019). Within the growing egg chamber, the growth of the nurse cells, their nuclei, and nucleoli is similar, which leads to isometrically scaling of these structures (Diegmiller et al., 2021; Imran Alsous et al., 2017). Similar isometric scaling of nuclear, nucleolar size, and cell size within the developing *C. elegans* intestine has also been observed (Uppaluri et al., 2016). Nurse cell nuclear growth is primarily due to multiple rounds of endoreplication, and increased

ploidy correlates with increased cell size (Diegmiller et al., 2021; Doherty et al., 2021; Orr-Weaver, 2015; Øvrebø and Edgar, 2018). Although all nurse cells and their nuclei grow during oogenesis, it has recently been demonstrated that nurse cell size is not uniform within the germ cell cluster; instead, there is a size hierarchy based on distance from the oocyte. The four posterior nurse cells directly connected to the oocyte are the largest, whereas the most anterior nurse cell that is four ring canals away from the oocyte is the smallest (Diegmiller et al., 2021; Imran Alsous et al., 2017). Therefore, within this system, we have the opportunity to monitor subcellular scaling in a growing tissue with a cell size gradient.

The germline ring canals are essential structures whose size must be tightly regulated to produce a viable mature egg. The germ cell cluster is formed through four rounds of mitosis followed by incomplete cytokinesis. These mitotic divisions are synchronous across the cluster, which gives rise to a stereotypical pattern of connections (Fig. 1A,E). After the four mitotic divisions have completed, the ring canals begin to expand (Ong and Tan, 2010), ultimately reaching a final diameter of nearly 10 µm. Although it is known that ring canal growth is required for fertility, the scaling of ring canal size during oogenesis has not been determined.

Here, we characterize the scaling of two types of ring canals: the four ring canals that connect the most posterior nurse cells to the oocyte and the most anterior ring canal. We hypothesized that ring canal size and growth would correlate with that of the associated nurse cells; if that were true, we would have expected to see an anterior-posterior gradient in ring canal size and growth. Instead, our data supported an alternative hypothesis that ring canal growth is most closely linked to lineage. The largest, “first born” ring canals grew more slowly compared to smaller ring canals that are derived from subsequent mitotic divisions. This scaling pattern is maintained even if polarized transport is reduced, initial ring canal size is altered, or if germ cells go through an additional mitotic division. Our lineage analysis also revealed a novel aspect of nurse cell nuclear growth; the nuclei of nurse cells formed during the first mitotic divisions grow faster than those formed during subsequent divisions. Finally, analysis of a set of artificially selected “big egg” and “small egg” lines suggests that subtle changes to ring canal scaling could provide a mechanism to regulate final egg size.

Materials and Methods

Fly Stocks and Maintenance: Flies were maintained on a cornmeal molasses diet at 18-25°C. The "big egg" and "small egg" *D. melanogaster* lines were obtained from C. Miles (Augustana University)(Jha et al., 2015; Miles et al., 2011). The following lines were obtained from the Bloomington *Drosophila* stock center: w^{1118} (BDSC# 3605), *UAS-dhc64C-RNAi* (BDSC #36583), *matαTub-GAL4* (BDSC #7063), maternal triple driver MTD-GAL4 (BDSC #31777), *nos-GAL4* (BDSC #32563), *UAS-arpC2-RNAi* (BDSC #43132), and *UAS-CG34200-RNAi* (BDSC #44463).

Immunofluorescence and Imaging: Female flies were maintained with ground yeast in the presence of males for ~48-60 hours prior to dissection. Ovaries were dissected in Schneider's media, fixed in 4% formaldehyde, and stained with an HtsRC antibody (1:20, hts RC DSHB), phalloidin (1:500; either TRITC or FITC conjugated; ECM Biosciences), and DAPI (1:500). Anti-mouse secondary antibodies were used at a 1:200 dilution (Jackson Immunolab). Tissue was imaged using a Nikon Ti2-E Inverted microscope equipped with a Yokogawa CSU-X1 Spinning Disk and Hamamatsu ORCA Fusion camera with a 20x PLAN APO objective. Although we tried to be consistent in scaling confocal images in the figures, there were differences in fluorescence intensity within z-stacks, so scaling was adjusted to best highlight the structures of interest in each image.

Mature Egg Collection and Volume Measurements: Male and female flies were incubated with ground yeast for approximately 24 hours at 25°C prior to transferring them to cages with apple juice plates and wet yeast. Mature eggs were collected and imaged using a Zeiss LP-520 and ProgRes MF camera (Jenoptik) using ProgRes Capture Pro Software (Jenoptik). Length and width measurements were made using Fiji or ImageJ, and volumes were calculated using the formula: Volume = $1/6*\pi*\text{Width}^2*\text{Length}$.

Ring canal and Nuclear Measurements: Ring canal diameter was measured from the HtsRC stain using the line tool in Fiji/ImageJ. Nuclear areas were measured using the

freehand drawing tool to trace around the outside of the DAPI stain. Graphing and statistical analyses were performed using Prism 10 (GraphPad Software, LLC).

Results

Ring canal scaling is related to lineage

It has recently been shown that there is a size hierarchy within the germ cell cluster; the largest nurse cell nuclei are located at the posterior, whereas the smallest nuclei are within the most anterior nurse cell (Diegmiller et al., 2021; Imran Alsous et al., 2017). Because nuclear growth has been shown to be tightly coupled to cell growth (Diegmiller et al., 2021), we can use nuclear size as a proxy for nurse cell size.

We first wanted to determine whether there were differences in the growth rate of nurse cell nuclei in different regions of the germ cell cluster. We focused our analysis on two sets of nurse cells – the four posterior nurse cells that are directly connected to the oocyte and the most anterior nurse cell (Fig. 1E). This should allow us to compare the relative growth rates of the largest and smallest nurse cells. We found that as the egg chamber increases in volume, the anterior and posterior nurse cell nuclei also increase in size, but at slightly different rates (Fig. 1A,B). If we plot these measurements on a log-log scale, then isometric scaling would be reflected by a slope of approximately 2/3 or 0.666; a smaller slope would indicate hypoallometric scaling, and a higher slope would indicate hyperallometric scaling. We found that the posterior nuclei scale nearly isometrically with egg chamber volume (Fig. 1B; scaling exponent of 0.652, 95% confidence interval is 0.6269-0.6777), which is consistent with what has been previously shown (Diegmiller et al., 2021). In contrast, the nuclei in the most anterior nurse cell scales slightly hypoallometrically (Fig. 1B; scaling exponent of 0.626, 95% confidence interval of 0.5925-0.6595, $p>0.05$). The y-intercepts of these two lines are significantly different (Fig. 1B; $p<0.0001$), which is consistent with the smaller size of the anterior cells (and their nuclei) that has been previously reported. This suggests that in addition to absolute differences in nuclear size, there could be modest differences in nurse cell (and nuclear) growth rates based on position within the germ cell cluster.

If we hypothesize that ring canal growth correlates with nurse cell size and growth, then we would predict that the posterior ring canals should be larger and grow

faster than the anterior ring canals. We measured the diameter of the ring canals that connect the same nurse cells to either the oocyte (for the posterior ring canals) or to another nurse cell (for the anterior ring canal). There was no difference in the scaling exponent between these two ring canal types (Fig. 1C; 95% confidence interval of 0.2180-0.2414 for the posterior ring canals and 0.2089-0.2504 for the anterior ring canals), but there was again a significant difference in the y-intercepts (Fig. 1C; $p<0.0001$), which reflects the smaller size of the anterior nuclei. At first glance, these data appeared to support our hypothesis.

However, what was obvious from our analysis was that the size of the four posterior ring canals varied significantly within an egg chamber (Fig. 1A,C). This variation in size could be explained by the emergence of one ring canal at the end of each of the four mitotic divisions that form the germ cell cyst. It has been shown that the ring canals formed during the earlier mitotic divisions are larger than those that are formed during the later divisions (Ong and Tan, 2010), at least within the germarium. Therefore, we hypothesized that lineage could be the source of the ring canal size differences. If we separate out the posterior ring canals based on their mitotic division of origin (Fig. 1E; M1 for the first mitotic division, M2 for the second mitotic division, etc.), we found that the “first born” M1 ring canals were nearly always the largest, whereas the “youngest” M4 ring canals were typically the smallest (Fig. 1A,D). In addition to these size differences, the posterior ring canals had different scaling exponents; the M1 ring canals had a significantly lower scaling exponent compared to the M4 ring canals (M1 ring canals: 0.2018, 95% confidence interval 0.1879-0.2157; M4 ring canals: 0.2523, 95% confidence interval 0.2338-0.2707). Further, the scaling exponent for the anterior ring canals, which are also formed during the fourth mitotic division, was not significantly different from that of the posterior M4 ring canals (Fig. 1D). This observation suggests that ring canal size and growth are not linked to nurse cell size, since the anterior nurse cells are the smallest and grow more slowly than the posterior nurse cells. Instead, our data support the hypothesis that ring canals scale differently based on their lineage. We hypothesized that these differences could reflect a need for the initially smaller M4 ring canals to grow more quickly to try to “catch up” to the size of the larger M1 ring canals.

Reducing directed transport reduces ring canal size and leads to a modest increase in scaling

Ring canals serve a specific purpose within the egg chamber by providing a channel for the directed transport of material from the nurse cells into the oocyte. Based on the observed size differences, we hypothesized that the larger M1 ring canals may allow more material to flow through them than the smaller M4 ring canals; this difference in flow could provide a mechanism to drive faster growth of the M4 ring canals. If the amount of directed transport through the ring canal inversely correlates with ring canal growth, then reducing transport should increase growth. It has been shown that the amount of biased transport of materials through the germline ring canals correlates with their position along the anterior-posterior axis. Movement of materials through the anterior ring canals is bidirectional, whereas the movement through the posterior ring canals is significantly biased toward the oocyte. Depletion of the linker protein, Short stop (Shot), or dynein heavy chain (Dhc64C), significantly reduced the biased transport at the posterior, which reduced oocyte size (Lu et al., 2021). Therefore, if ring canal size scaling is sensitive to transport through the posterior ring canals, then depletion of Dhc64C should alter the scaling exponents.

We first confirmed that depletion of Dhc64C led to a significant reduction in oocyte size. To perform the depletion, we used *matαTub-GAL4,* which bypasses the requirement for dynein during earlier stages of oogenesis (Lu et al., 2022; McGrail and Hays, 1997). This phenotype was most obvious during mid-oogenesis (stage ~5-8), so we focused our analysis on these egg chambers (Fig. 2A,B). In the *dhc64C-RNAi* egg chambers, the posterior nuclei tended to be smaller than in control (y-intercept was significantly different), and although the scaling exponent was higher, this difference was not significant (Fig. 2C, 95% confidence interval of 0.6755-0.7407 for control compared to 0.6793-0.8475 for *dhc64C-RNAi*, $p>0.05$). For the anterior nuclei, we did not expect to see a difference in nuclear size or scaling, since these cells were four ring canals away from the oocyte, and ring canal transport has been reported to be more bidirectional. Instead, we observed a significant reduction in the scaling exponent, leading to hypoallometric scaling (Fig. 2C; Control: 0.6856, 95% confidence interval of

0.6416-0.7296; *dhc64C-RNAi:* 0.5060, 95% confidence interval of 0.3929-0.6192). This suggests that when directed transport is reduced, nurse cells respond differently (or are impacted in different ways) depending on their proximity to the oocyte.

Next, we performed the same analysis of ring canal diameter in the control and *dhc64C-RNAi* egg chambers. We found that depletion of Dhc64C led to a significant decrease in ring canal diameter, and there was a modest, but not significant increase in ring canal growth rate (Fig. 2D; y-intercepts for both ring canal types were significantly different). A similar reduction in ring canal size was observed in Shot-depleted egg chambers (Lu et al., 2021). If we separated the ring canals based on mitotic division of origin, we again found that depletion of Dhc64C led to a consistent increase in the growth rate for all ring canal types (Fig. 2E, scaling exponents were not significantly different $p>0.05$, but there was a significant difference in y-intercepts for control/*dhc64C-RNAi* comparisons for M2, M3, M4 and the anterior ring canals, $p<0.05$). These data show that reducing dynein-mediated transport led to a modest, yet consistent reduction in ring canal size and increase in scaling. However, despite these changes, the pattern of lineage-based size scaling was maintained.

Increasing initial ring canal size does not dramatically alter scaling

Thus far, our data could support a role for ring canal size and/or lineage in determining scaling. If ring canal size inversely correlates with scaling, then increasing initial ring canal diameter should reduce the scaling exponent. We have previously shown that depletion of the ArpC2 subunit of the Arp2/3 complex led to a significant increase in ring canal diameter during early stages of oogenesis (Thestrup et al., 2020). By mid- to late-oogenesis, these egg chambers contain a large number of smaller, and even lumen-less ring canals connecting nurse cells to each other (Fig. 3A; (Hudson and Cooley, 2002; Thestrup et al., 2020), but the posterior ring canals are typically more stable and can therefore be used to determine the effect of this depletion on ring canal scaling.

Based on our previous study, we expected that the ring canals in the ArpC2-depleted egg chambers would initially be larger than controls. When we separated ring canals based on their mitotic division of origin, we found that in the *arpC2-RNAi* egg

chambers, the ring canals tended to be larger than those in similarly-sized control egg chambers (Fig. 3B,S1A). If ring canal size impacts scaling, then these ring canals should have a smaller scaling exponent than lineage-matched controls. Our analysis showed that there was a consistent, but not significant decrease in the scaling exponents for the *arpC2-RNAi* egg chambers compared to controls (Fig. 3B,C, S1A; the y-intercepts were significantly different in all pairwise comparisons, $p<0.05$). Again, despite the changes in ring canal size, the pattern of lineage-based scaling was maintained in the *arpC2-RNAi* egg chambers (Fig. 3C; scaling exponent increased from M1 to M4). This suggests that although initial ring canal size could have a modest impact on growth, lineage may still provide the strongest indicator of scaling.

While measuring ring canals in the *arpC2-RNAi* egg chambers, we noticed that the nuclei in the posterior nurse cells seemed larger than in the control egg chambers. Although there was no significant difference in the scaling exponent for the posterior nuclei, the *arpC2-RNAi* egg chambers contained larger nuclei than similarly sized control egg chambers. This relative increase in posterior nuclear size in the *arpC2-RNAi* egg chambers motivated us to further explore this phenotype by separating the nuclear measurements based on mitotic division of origin. We found that for all types, the *arpC2-RNAi* egg chambers contained larger nuclei than controls (Fig. S1B; shown by differences in y-intercepts $p<0.0001$); we did find that the scaling exponent was consistently smaller in *arpC2-RNAi* egg chambers, but these differences were not significant (Fig. 3D). In these egg chambers, we also often observed a very small nurse cell directly connected to one of these larger posterior nurse cells (Fig. 3A arrow). Although additional experiments are required to further explore the relationship between ring canal size and nurse cell growth, it raises the possibility that the posterior cells are enlarging at the expense of other cells in the cluster.

The lineage-based analysis also allowed us to appreciate an interesting pattern in the scaling of the different types of posterior nuclei in control egg chambers. Specifically, we found that the M1 nuclei had a higher scaling exponent than the nuclei that were formed during subsequent mitotic divisions (Fig. 3D,S1B). Although the nuclei in the *arpC2-RNAi* egg chambers were significantly larger than in control, they showed a similar pattern of decreasing scaling exponent based on birth order (Fig. 3D). With this

nuclear lineage data, we could also compare ring canal size to nuclear size. Relative to nurse cell nuclear growth (which could be used as a proxy for nurse cell growth), the older M1 ring canals grew more slowly than the ring canals that are derived from the later divisions (Fig. 3E). This again confirms the significant, lineage-based differences in the growth of the posterior nurse cells and the ring canals that connect them to the oocyte.

Lineage-based ring canal and nuclear scaling is maintained in egg chambers that have undergone an additional mitotic division

Thus far, we have described previously unappreciated trends in the size scaling relationships of the germline ring canals and nurse cell nuclei based on mitotic division of origin. Although size may contribute to the growth differences, lineage seems to be the most consistent predictor of scaling. To further test this relationship, we turned to a condition in which the germ cells undergo an additional (fifth) mitotic division. As part of another project, it was found that when a shRNA construct (P{TRiP.GLC01618}attP2) was used to target the depletion of CG34200 using *nanos-GAL4*, a large number of egg chambers contain 31 nurse cells and ring canals, with a single oocyte connected to five posterior nurse cells (Fig. 4A). This indicates that an extra round of mitotic division with incomplete cytokinesis occurred in these cysts. Because of this phenotype, we have named CG34200 *double fission* (*dubf*). Additional work to further characterize the *dubf* depletion phenotype is in progress (manuscript in preparation), but we could use this condition to determine whether nuclear and ring canal scaling changes when there is an additional mitotic division.

For the controls, we observed the same pattern of nuclear scaling and ring canal scaling; the nuclear scaling exponent decreased (Fig. 4B,D), whereas the ring canal scaling exponent increased (Fig. 4E,G) from M1-M4. When Dubf was depleted from the germline and an additional round of mitosis produced a fifth posterior ring canal, we saw similar trends for both nuclear and ring canal scaling. The nuclear scaling exponent decreased from M1 to M5, whereas the ring canal scaling exponent increased from M1 to M5 (Fig. 4B-G). If we looked at ring canal size based on lineage, we found that the ring canals in *dubf-RNAi* egg chambers were typically larger (*data not shown*) and had a

higher scaling exponent (Fig. 4G) compared to controls, which suggests that ring canal size does not always determine scaling. Therefore, this finding again supports the model that lineage is the strongest predictor of ring canal scaling.

Scaling differences were observed across a collection of "big" and "small" egg lines

When considering the functional role of size scaling of the germline ring canals and connected nurse cells, an obvious question was whether altering either could provide a mechanism to ultimately impact final egg size. Therefore, we chose to monitor scaling within a collection of *D. melanogaster* lines that were artificially selected to produce either "big" or "small" eggs (Jha et al., 2015; Miles et al., 2011). We first confirmed that these lines still produce significantly larger or smaller mature eggs; all the "big egg" lines produced significantly larger mature eggs than all the "small egg" lines (Fig. 5A; $p<0.0001$ ANOVA with Tukey's post-hoc). From this collection, we performed further analysis on two of the "big egg" lines (1.40.1 and 3.34.1) and two of the "small egg" lines (7.17.4 and 9.31.4).

We hypothesized that changes in the size or scaling of the posterior ring canals would have the most direct effect on oocyte and final egg size. After completing these measurements, we observed some differences in posterior ring canal scaling across the four lines (Fig. 5B). If we split out the ring canals based on mitotic division of origin, we found that the lineage-based pattern of scaling exponents followed what we had observed with the controls. The scaling exponents typically increased from M1 to M4 (Fig. 5C), and within each line, there was no significant difference in the scaling exponent for the M4 ring canal compared to the anterior ring canal (Fig. 5C). When we compared the scaling exponents across the four lines, there were significant differences for M1, M2, and M4; however, only one of the "small egg" lines (7.17.4) consistently had scaling exponents that were lower than the "big egg" lines (Fig. 5C). These data demonstrate that the effect of lineage on ring canal scaling is conserved, and it suggests that at least in one line, reducing posterior ring canal scaling could provide a mechanism to produce a smaller mature egg.

For the combined posterior nuclei, we found that there were significant differences in the scaling exponents between the different lines. All but one of the

pairwise comparisons yielded significant differences in the scaling exponents (Fig. 5D; the scaling exponent for 3.34.1 was not significantly different from that of 9.31.4). If we separated nuclei based on their lineage (Fig. 5E), we found that one “big egg” line consistently had a higher scaling exponent (1.40.1), and one “small egg” line consistently had a lower scaling exponent (7.17.4). This suggests that changes in nurse cell (nuclear) growth could also contribute to changes in final egg size.

Although we expected that the posterior structures would have the most direct impact on oocyte growth and mature egg size, we did want to determine the scaling of the anterior nuclei and ring canals. We did not notice a clear pattern in the anterior ring canal scaling exponent (Fig. S2A,B), but we did find that the “small egg” lines tended to have a lower anterior nuclear scaling exponent than the “big egg” lines, although the only significant difference was between lines 1.40.1 and 9.31.4 (Fig. S2A,C). This reduction in anterior nuclear scaling was reminiscent of the effect we observed following depletion of Dhc64C (Fig. 2C), and it led us to wonder whether this might be a response to or consequence of reduced transport into the oocyte in the small egg lines, which could ultimately reduce mature egg volume.

Discussion

We still have much to learn about how cells within developing tissues coordinate their size and the size and number of their subcellular structures. Here, we have characterized size scaling of the germline ring canals within the developing egg chamber. Our data support the model that birth order inversely correlates with ring canal growth; the larger, “older” ring canals show a lower scaling exponent than the smaller, “younger” ring canals (Fig. 1-4). Although some data support a modest effect of directed transport (Fig. 2) or initial ring canal size (Fig. 3), lineage consistently provided the strongest predictor of ring canal scaling. Analysis of artificially selected lines that produce eggs of different sizes (Fig. 5) suggests that altering posterior ring canal scaling could provide a mechanism to adjust final egg size. Our lineage analysis also revealed that nurse cell nuclear growth was impacted by birth order. The “oldest” nurse cells contain nuclei that grow faster than the “younger” nurse cells (Fig. 3,4).

Ring Canal Scaling

Although ring canals are known to undergo significant growth during oogenesis, to our knowledge, this is the first time that their scaling has been described. It was not surprising that the diameter of the ring canals would increase more slowly than other structures within the egg chamber, such as the nurse cell nuclei or nucleoli (Diegmiller et al., 2021). Although they are a common feature of developing germ cells across the animal kingdom, most intercellular bridges are much smaller (typically less than 2 μm in diameter) than the germline ring canals within the egg chamber (Haglund et al., 2011). A recent study reported that when they are formed, the ratio of intercellular bridge diameter to cell diameter was ~5-15% (Singh et al., 2022), which suggests that there might be a physical limit to the size of a stable intercellular bridge. One way to overcome this limitation might be to alter ring canal structure. Most other intercellular bridges contain a single "rim," but the germline ring canals within the egg chamber, which undergo a nearly 20-fold increase in diameter, contain two (Haglund et al., 2011). Perhaps this more complex structure provides a mechanism to enable more growth than other intercellular bridges or to stabilize these larger channels.

During their formation, ring canals differ in size due to differences in the degree of contractile ring constriction at the end of each mitosis, producing smaller ring canals with each round of division (Ong 2010). It has been shown that once the mitotic divisions are complete, the M1 ring canal is the first to initiate the growth phase (Ong 2010), and we assumed that growth would be similar for all ring canal types. Instead, our data support a lineage-based effect on ring canal scaling, with the "oldest" ring canals growing more slowly than the "younger" ring canals (Fig. 1-5). It is interesting to speculate about what might lead to these differences in ring canal growth rates. The scaling differences could reflect nurse cell size differences; however, if that were the case, then the posterior M4 ring canal would scale differently than the anterior ring canal, since the anterior cells (and their nuclei) are always smaller than the posterior cells (Diegmiller 2021; Fig. 1). However, the observation that the scaling exponents for the M4 posterior ring canal and the anterior ring canal were not significantly different (Fig. 1) argues against that model.

Another possibility is that there could be structural differences in the ring canals that are formed during the different mitotic divisions. Early work suggests that the germ cells do not double in size between each round of mitosis (Koch and King, 1966), so as the cluster develops, the dividing cells are smaller and smaller. It has been shown that in the *C. elegans* embryo, the contractile ring contains structural memory of cell size; the contractile rings in larger cells divide faster than those in smaller cells. This structural memory has been proposed to be due to the incorporation of different numbers of contractile units into rings of different sizes (Carvalho et al., 2009). Because the ring canal develops from the contractile ring following incomplete cytokinesis, it is possible that the structure of the nascent intercellular bridge may retain some memory of the size of the dividing cell, which may then impact its subsequent rate of growth. Depletion of ArpC2 has been previously shown to increase ring canal size in early oogenesis (Thestrup et al., 2020), and here we found that there was a modest reduction in posterior ring canal scaling in these egg chambers (Fig. 3). Additional work is required to further explore the relationship between initial ring canal size and subsequent growth and to determine the mechanisms that lead to the very small ring canals observed during later oogenesis (Hudson and Cooley, 2002; Thestrup et al., 2020). Alternatively, if the M1 contractile ring constricts less than contractile rings formed in subsequent divisions, perhaps it must be reinforced by the recruitment of more actin filaments or stabilized by additional cell-cell junctions, which may impact growth. Extensive cell-cell contacts have been observed in the developing germ cell cysts (Loyer et al., 2015; Riparbelli et al., 2022; Tilney et al., 1996), but a comparison of their distribution within different regions of the germ cell cluster has not been performed.

One final explanation we considered is that the growth of a posterior ring canal could depend on how many other ring canals exist within that germ cell. For example, the M1 ring canal that we were monitoring is connecting the oocyte to a nurse cell that contains three additional ring canals (M2, M3, and M4 types), whereas the posterior M4 ring canal is the only intercellular bridge for that nurse cell (Fig. 1E). Therefore, the differences in growth rates could be due to the presence or absence of additional ring canals within that cell. One argument against that model is that in Dubf-depleted egg chambers that had undergone an additional round of mitosis, each of the posterior

nurse cells had an additional ring canal, but the scaling exponents were higher than what we observed in the controls (Fig. 4). Therefore, additional work is necessary to determine the molecular mechanisms underlying these scaling differences.

Nuclear Scaling

Another surprising outcome of this analysis was that there were also differences in nuclear size scaling based on birth order, but that they were the opposite of what we observed for the ring canals. Specifically, the posterior M1 nuclei had the highest scaling exponent, and the M4 nuclei had the lowest scaling exponent. Posterior nuclei are larger than anterior nuclei (Alsous et al., 2017; Diegmiller et al., 2021), and nurse cell ploidy shows a similar hierarchy based on distance from the oocyte. It has been proposed that translation of the cell cycle regulator, Dacapo, in the oocyte and its diffusion back into the nurse cells could partially explain the difference in endocycle number within the germ cell cluster (Doherty et al., 2021). If the larger M1 ring canals allow more of this regulator to diffuse back into the M1 nurse cells, then this could explain why these nuclei may grow faster than nuclei within cells connected by smaller ring canals.

Nurse cell growth could also depend on the number of additional connections that nurse cell has to other nurse cells. Because nuclear size can be used as a reasonable proxy for cell size (Alsous et al., 2017; Diegmiller et al., 2021), it would suggest that the M1 nurse cell is growing the fastest and the M4 nurse cell grows the slowest. Could it be that delivery of cytoplasmic factors from three other nurse cells enhances the growth rate of the M1 nurse cell? In multinucleate fission yeast, the cytoplasmic environment affects nuclear growth; nuclei that were surrounded by a larger cytoplasmic volume grew faster than those that were more closely spaced (Neumann and Nurse, 2007). In the Dubf-depleted egg chambers, where the posterior nurse cells are each connected to an additional nurse cell (Fig. 4), there was a significant increase in the nuclear scaling exponent compared to controls, which would support that model. In the ArpC2-depleted egg chambers, the posterior nurse cells were typically larger and contained larger nuclei than the controls, but we often observed very small nurse cells connected to these posterior cells by very small ring canals (Fig. 3). If there is a signal,

such as Dacapo, that diffuses from the oocyte into the nurse cells to promote endocycling (Doherty et al., 2021), then these small ring canals may significantly reduce or prevent the anterior diffusion of that signal. Additional experiments could further explore how the size of ring canals anterior or posterior to a given nurse cell could impact their size and growth or explore whether differences in nuclear import/export, which also impacts nuclear size (Levy and Heald, 2012), could explain the nuclear size scaling that we observed.

Changes in scaling could generate eggs of different sizes

Final egg size is likely determined by many genes that impact the size or growth of multiple structures during oogenesis. One way to alter final egg size could be to increase or decrease ring canal scaling, which could then affect the directed transfer of materials into the oocyte, ultimately changing final egg size. Whole genome sequencing of the entire collection of artificially selected “big egg” and “small egg” lines identified a set of candidate genes that may contribute to egg size evolution (Jha et al., 2015); that list included many that localize to the germline ring canals or have been implicated in ring canal size regulation, including Cheerio/Filamin, Flapwing, Mbs, and Short stop (Jha et al., 2015). Cheerio/Filamin, localizes to germline ring canals and is required for formation of the actin-rich inner rim (Robinson et al., 1997). Flapwing and Mbs have been shown to work together to inhibit myosin activity during incomplete cytokinesis, and mutants form smaller ring canals (Ong et al., 2010; Yamamoto et al., 2013), and as previously discussed, Short stop is a linker protein that promotes directed transport into the oocyte (Lu et al., 2021). One of the small egg lines (7.17.4) consistently had a lower scaling exponent for all posterior ring canals (Fig. 5), which suggests that this could be a mechanism to alter final egg size.

Additional studies will be necessary to confirm the connection between ring canal scaling and final egg size. Because our study looked at a fairly narrow range of final egg sizes, future work could expand to include analysis of oogenesis in insects that produce much larger and much smaller eggs.

Figure Legends

Figure 1: Ring canal size and nuclear size vary within the egg chamber. (A) Single plane confocal images of control egg chambers (*w^{1118}/+;;matαTub-GAL4*) stained with an HtsRC antibody, phalloidin, and DAPI. Panels below show anterior, M4, and M1 ring canals from each of the indicated egg chambers (which were located in different z-planes than the one shown in the larger panels); ring canal identity is indicated by the colored bars, which match those used in (E). Measurements of these ring canals and associated nuclei are included below; measurements were made in the z-plane where each structure was in focus. Scale bars are 5 µm. (B-D) log-log plots of egg chamber volume, nuclear area, or ring canal diameter from stage 6-10b. Error bars in B,C are standard deviation. n=61 egg chambers. 95% confidence intervals are shown. (E) Cartoon showing the stereotypical connections that result from the four rounds of mitotic divisions. Fill colors correspond to those used in D, and the thickness of the outlines and connecting lines correspond to distance from the oocyte (thicker lines are closer to the oocyte, and thinner lines are further from the oocyte).

Figure 2: Reducing oocyte growth has a modest effect on ring canal size and scaling. (A) Single plane confocal images of control and *dhc64C-RNAi* egg chambers (*matαTub-GAL4*) stained with an HtsRC antibody, phalloidin, and DAPI. (B-D) log-log plots of egg chamber volume, oocyte area, nuclear area, or ring canal diameter from stage 6-10b. Error bars in C,D are standard deviation. 95% confidence intervals are shown. (E) Scaling exponent (+/- 95% confidence interval) for ring canals separated by lineage. n=49 egg chambers for control and 28 egg chambers for *dhc64C-RNAi*.

Figure 3: Depletion of the Arp2/3 complex subunit, ArpC2, does not affect lineage-based scaling. (A) Single plane confocal images of control and *arpC2-RNAi* egg chambers (*MTD-GAL4*) stained with an HtsRC antibody, phalloidin, and DAPI. Arrow points to smaller nucleus within a nurse cell connected to a larger posterior nurse cell. (B) log-log plot of egg chamber volume and ring canal diameter from stage 6-10b. (C,D) Scaling exponent (+/- 95% confidence interval) for ring canals (C) or nuclei (D)

separated by lineage. (E) log-log plot of posterior nuclear area and ring canal diameter (separated by lineage) in control egg chambers from stage 6-10b. 95% confidence intervals are shown. n=61 egg chambers for control and 61 egg chambers for *arpC2-RNAi*.

Figure 4: Depletion of Double Fission (Dubf) increases the number of germ cell divisions but does not alter the pattern of ring canal and nuclear scaling. (A) Single plane confocal images of control and *dubf-RNAi* egg chambers (*nos-GAL4*) stained with an HtsRC antibody, phalloidin, and DAPI. Maximum intensity projections of the *dubf-RNAi* egg chambers are included to show the extra ring canals in these egg chambers. log-log plots of egg chamber volume, nuclear area (B,C), or ring canal diameter (E,F) from stage 6-10b. n=74 egg chambers for control and 64 egg chambers for *dubf-RNAi*. 95% confidence intervals are shown. (D,G) Scaling exponent (+/- 95% confidence interval) for nuclei (D) or ring canals (G) separated by lineage

Figure 5: Changes in posterior ring canal and nuclear scaling in "big egg" and "small egg" *D. melanogaster* lines. (A) Box and whiskers plot (10-90th percentile) of mature egg volume of "big egg" and "small egg" *D. melanogaster* lines. One-way ANOVA with Tukey's multiple comparisons test indicates mature eggs from all "big egg" lines (9.31.4, 8.26.2, 8.11.1, 7.17.4, and 9.2.2) are significantly bigger than all "small egg" lines (1.16.1, 2.15.4, 2.49.3, 1.40.1, and 3.34.1) ($p<0.05$). n= 35-77 eggs per line. (B,D) log-log plots of ring canal diameter and nuclear area in two "big egg" (1.40.1 and 3.34.1) and two "small egg" lines (7.17.4 and 9.31.4). 95% confidence intervals are shown. (C,E) Scaling exponent (+/- 95% confidence interval) for ring canals (C) or nuclei (E) separated by lineage. n=29 egg chambers for 1.40.1, 46 egg chambers for 3.34.1, 44 egg chambers for 7.17.4, and 43 egg chambers for 9.31.4.

Figure S1: Depletion of ArpC2 increases the size of the posterior nuclei. (A) log-log plot comparing egg chamber volume and posterior ring canal diameter. Error bars are standard deviation, and 95% confidence intervals are shown. (B) log-log plot comparing egg chamber volume and nuclear area (separated by mitotic division of

origin, M1-M4) from stage 6-10b. n=61 egg chambers for control and 61 egg chambers for *arpC2-RNAi*.

Figure S2: Changes in anterior ring canal and nuclear scaling in "big egg" and "small egg" *D. melanogaster* lines. (A) Table with the slopes and y-intercepts of the linear regressions generated from log-log plots of data based on cell type (M1-M4 posterior or anterior). (B,C) log-log plots of egg chamber volume and (B) anterior ring canal diameter or (C) anterior nuclear area in two big egg (1.40.1 and 3.34.1) and two small egg lines (7.17.4 and 9.31.4). n=29 egg chambers for 1.40.1, 46 egg chambers for 3.34.1, 44 egg chambers for 7.17.4, and 43 egg chambers for 9.31.4.

.

Acknowledgements:

We would like to thank Seth Donoghue for helpful suggestions on the manuscript and Cecelia Miles for the big and small egg lines. This work was supported by the National Institutes of Health (NIH R15HD084243 to LL and R15GM099054 to WG). Stocks obtained from the Bloomington Drosophila Stock Center (NIH P40OD018537) were used in this study. The following antibody was obtained from the Developmental Studies Hybridoma Bank, created by the NICHD of the NIH and maintained at The University of Iowa, Department of Biology, Iowa City, IA 52242: hts RC antibody developed by L. Cooley.

References:

Ali-Murthy, Z., Fetter, R.D., Wang, W., Yang, B., Royer, L.A., Kornberg, T.B., 2021. Elimination of nurse cell nuclei that shuttle into oocytes during oogenesis. *J. Cell Biol*. 220, e202012101. https://doi.org/10.1083/jcb.202012101

Balachandra, S., Sarkar, S., Amodeo, A.A., 2022. The Nuclear-to-Cytoplasmic Ratio: Coupling DNA Content to Cell Size, Cell Cycle, and Biosynthetic Capacity. *Annu. Rev. Genet.* 56, 165–185. https://doi.org/10.1146/annurev-genet-080320-030537

Cantwell, H., Nurse, P., 2019. Unravelling nuclear size control. *Curr. Genet.* 65, 1281–1285. https://doi.org/10.1007/s00294-019-00999-3

Carvalho, A., Desai, A., Oegema, K., 2009. Structural Memory in the Contractile Ring Makes the Duration of Cytokinesis Independent of Cell Size. *Cell* 137, 926–937. https://doi.org/10.1016/j.cell.2009.03.021

Diegmiller, R., Doherty, C.A., Stern, T., Alsous, J.I., Shvartsman, S.Y., 2021. Size scaling in collective cell growth. *Development* dev.199663. https://doi.org/10.1242/dev.199663

Doherty, C.A., Diegmiller, R., Kapasiawala, M., Gavis, E.R., Shvartsman, S.Y., 2021. Coupled oscillators coordinate collective germline growth. *Dev. Cell* 56, 860-870.e8. https://doi.org/10.1016/j.devcel.2021.02.015

Gayon, J., 2000. History of the Concept of Allometry. *Am. Zool*. 40, 748–758. https://doi.org/10.1093/icb/40.5.748

Haglund, K., Nezis, I.P., Stenmark, H., 2011. Structure and functions of stable intercellular bridges formed by incomplete cytokinesis during development. *Commun. Integr. Biol.* 4, 1–9. https://doi.org/10.4161/cib.4.1.13550

Hudson, A.M., Cooley, L., 2002. A subset of dynamic actin rearrangements in Drosophila requires the Arp2/3 complex. *J. Cell Biol.* 156, 677–687. https://doi.org/10.1083/jcb.200109065

Huxley, J.S., Teissier, G., 1936. Terminology of Relative Growth. *Nature* 137, 780–781. https://doi.org/10.1038/137780b0

Imran Alsous, J., Villoutreix, P., Berezhkovskii, A.M., Shvartsman, S.Y., 2017. Collective Growth in a Small Cell Network. *Curr. Biol.* 27, 2670-2676.e4. https://doi.org/10.1016/j.cub.2017.07.038

Januschke, J., Gervais, L., Dass, S., Kaltschmidt, J.A., Lopez-Schier, H., Johnston, D.S., Brand, A.H., Roth, S., Guichet, A., 2002. Polar Transport in the Drosophila Oocyte Requires Dynein and Kinesin I Cooperation. *Curr. Biol.* 12, 1971–1981. https://doi.org/10.1016/S0960-9822(02)01302-7

Jha, A.R., Miles, C.M., Lippert, N.R., Brown, C.D., White, K.P., Kreitman, M., 2015. Whole-Genome Resequencing of Experimental Populations Reveals Polygenic Basis of Egg-Size Variation in *Drosophila melanogaster*. *Mol. Biol. Evol.* 32, 2616–2632. https://doi.org/10.1093/molbev/msv136

Koch, E.A., King, R.C., 1966. The origin and early differentiation of the egg chamber of Drosophila melanogaster. *J. Morphol.* 119, 283–303. https://doi.org/10.1002/jmor.1051190303

Levy, D.L., Heald, R., 2012. Mechanisms of intracellular scaling. *Annu. Rev. Cell Dev. Biol.* 28, 113–135. https://doi.org/10.1146/annurev-cellbio-092910-154158

Loyer, N., Kolotuev, I., Pinot, M., Le Borgne, R., 2015. *Drosophila* E-cadherin is required for the maintenance of ring canals anchoring to mechanically withstand tissue growth. *Proc. Natl. Acad. Sci.* 112, 12717–12722. https://doi.org/10.1073/pnas.1504455112

Lu, W., Lakonishok, M., Gelfand, V.I., 2021. Gatekeeper function for Short stop at the ring canals of the Drosophila ovary. *Curr. Biol*. 31, 3207-3220.e4. https://doi.org/10.1016/j.cub.2021.05.010

Lu, W., Lakonishok, M., Serpinskaya, A.S., Gelfand, V.I., 2022. A novel mechanism of bulk cytoplasmic transport by cortical dynein in Drosophila ovary. *eLife* 11, e75538. https://doi.org/10.7554/eLife.75538

Marshall, W.F., 2020. Scaling of subcellular structures. *Annu. Rev. Cell Dev. Biol.* 36, 219–236. https://doi.org/10.1146/annurev-cellbio-020520-113246

McGrail, M., Hays, T.S., 1997. The microtubule motor cytoplasmic dynein is required for spindle orientation during germline cell divisions and oocyte differentiation in Drosophila. *Development* 124, 2409–2419. https://doi.org/10.1242/dev.124.12.2409

Miles, C.M., Lott, S.E., Hendriks, C.L.L., Ludwig, M.Z., Manu, null, Williams, C.L., Kreitman, M., 2011. Artificial selection on egg size perturbs early pattern formation in Drosophila melanogaster. *Evol. Int. J. Org. Evol.* 65, 33–42. https://doi.org/10.1111/j.1558-5646.2010.01088.x

Neumann, F.R., Nurse, P., 2007. Nuclear size control in fission yeast. *J. Cell Biol.* 179, 593–600. https://doi.org/10.1083/jcb.200708054

Ong, S., Foote, C., Tan, C., 2010. Mutations of DMYPT cause over constriction of contractile rings and ring canals during Drosophila germline cyst formation. *Dev. Biol.* 346, 161–169. https://doi.org/10.1016/j.ydbio.2010.06.008

Ong, S., Tan, C., 2010. Germline cyst formation and incomplete cytokinesis during Drosophila melanogaster oogenesis. *Dev. Biol.* 337, 84–98. https://doi.org/10.1016/j.ydbio.2009.10.018

Orr-Weaver, T.L., 2015. When bigger is better: the role of polyploidy in organogenesis. *Trends Genet.* TIG 31, 307–315. https://doi.org/10.1016/j.tig.2015.03.011

Øvrebø, J.I., Edgar, B.A., 2018. Polyploidy in tissue homeostasis and regeneration. *Dev.* Camb. Engl. 145, dev156034. https://doi.org/10.1242/dev.156034

Riparbelli, M.G., Persico, V., Callaini, G., 2022. Cell-to-Cell Interactions during Early Drosophila Oogenesis: An Ultrastructural Analysis. *Cells* 11, 2658. https://doi.org/10.3390/cells11172658

Robinson, D.N., Smith-Leiker, T.A., Sokol, N.S., Hudson, A.M., Cooley, L., 1997. Formation of the Drosophila Ovarian Ring Canal Inner Rim Depends on Cheerio. *Genetics* 145, 1063–1072.

Singh, J., Imran Alsous, J., Garikipati, K., Shvartsman, S.Y., 2022. Mechanics of stabilized intercellular bridges. *Biophys. J.* 121, 3162–3171. https://doi.org/10.1016/j.bpj.2022.06.033

Thestrup, J., Tipold, M., Kindred, A., Stark, K., Curry, T., Lewellyn, L., 2020. The Arp2/3 complex and the formin, Diaphanous, are both required to regulate the size of germline ring canals in the developing egg chamber. *Dev. Biol.* 461, 75–85. https://doi.org/10.1016/j.ydbio.2020.01.007

Tilney, L.G., Tilney, M.S., Guild, G.M., 1996. Formation of actin filament bundles in the ring canals of developing Drosophila follicles. *J. Cell Biol.* 133, 61–74. https://doi.org/10.1083/jcb.133.1.61

Uppaluri, S., Weber, S.C., Brangwynne, C.P., 2016. Hierarchical Size Scaling during Multicellular Growth and Development. *Cell Rep.* 17, 345–352. https://doi.org/10.1016/j.celrep.2016.09.007

Yamamoto, S., Bayat, V., Bellen, H.J., Tan, C., 2013. Protein Phosphatase 1ß Limits Ring Canal Constriction during Drosophila Germline Cyst Formation. *PLOS ONE* 8, e70502. https://doi.org/10.1371/journal.pone.0070502

Figure 1

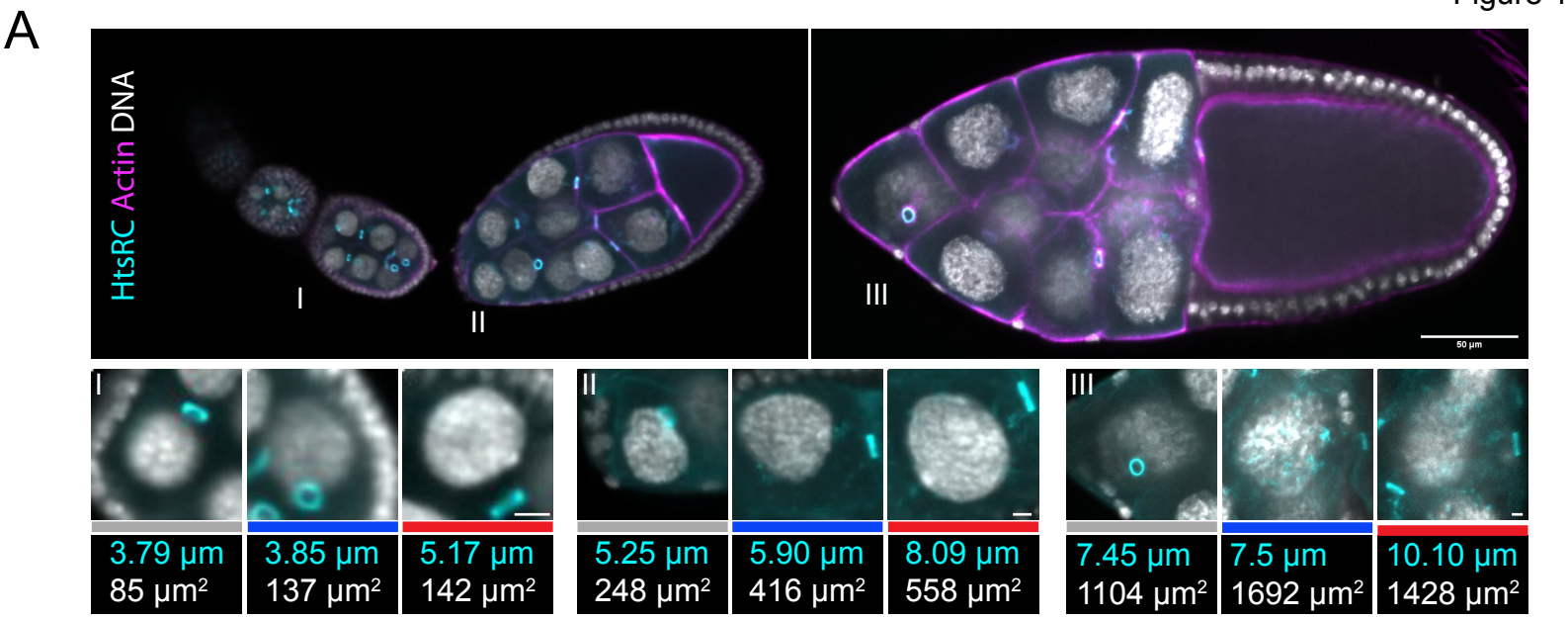
A
HtsRC Actin DNA
I
II
III
50 µm
3.79 µm
85 µm²
3.85 µm
137 µm²
5.17 µm
142 µm²
5.25 µm
248 µm²
5.90 µm
416 µm²
8.09 µm
558 µm²
7.45 µm
1104 µm²
7.5 µm
1692 µm²
10.10 µm
1428 µm²

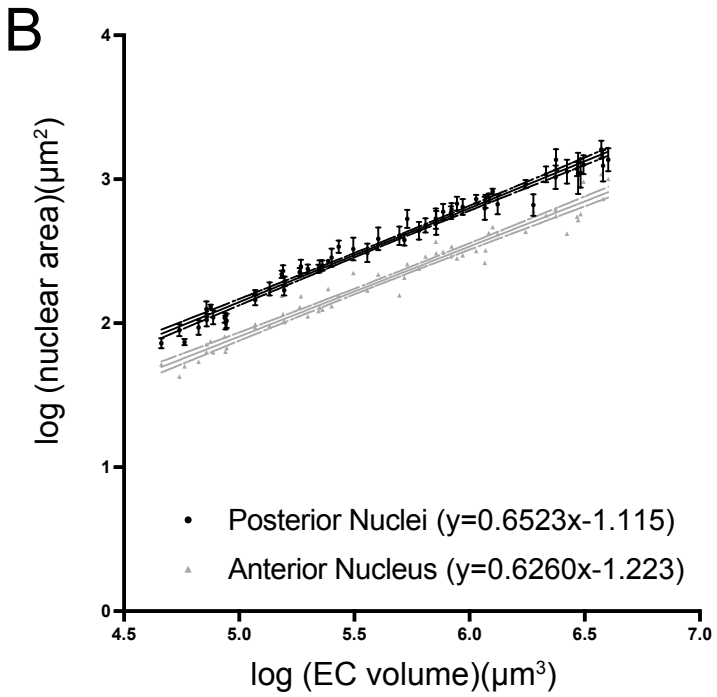
B
log (nuclear area)(µm²)
log (EC volume)(µm³)
Posterior Nuclei (y=0.6523x-1.115)
Anterior Nucleus (y=0.6260x-1.223)

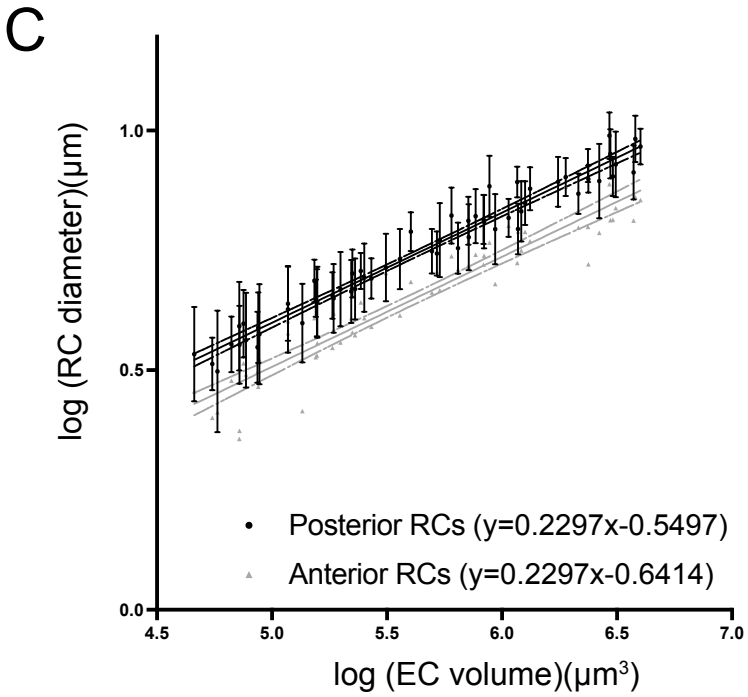
C
log (RC diameter)(µm)
log (EC volume)(µm³)
Posterior RCs (y=0.2297x-0.5497)
Anterior RCs (y=0.2297x-0.6414)

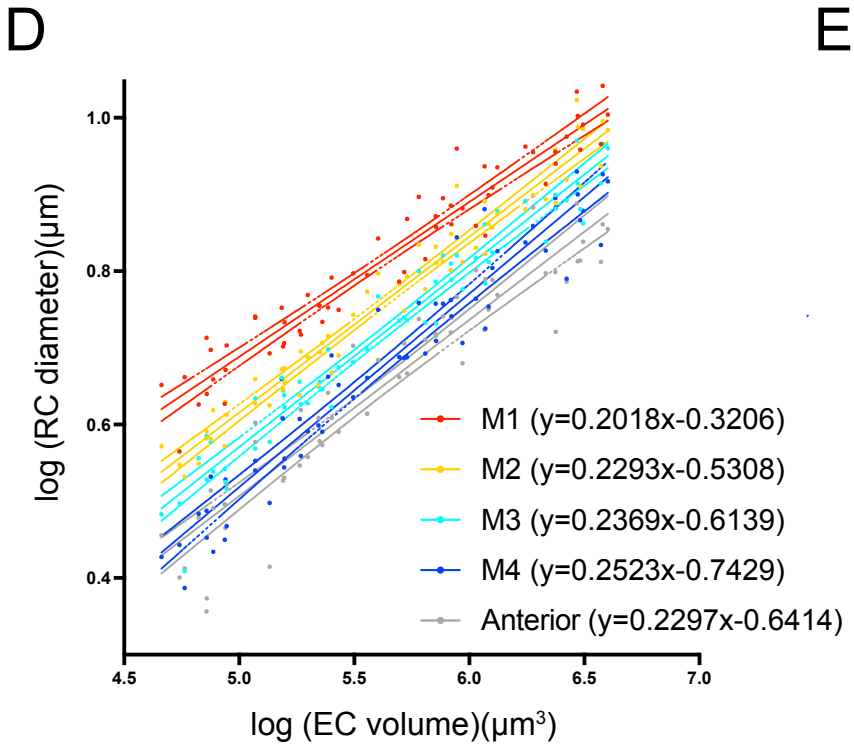
D
log (RC diameter)(µm)
log (EC volume)(µm³)
M1 (y=0.2018x-0.3206)
M2 (y=0.2293x-0.5308)
M3 (y=0.2369x-0.6139)
M4 (y=0.2523x-0.7429)
Anterior (y=0.2297x-0.6414)

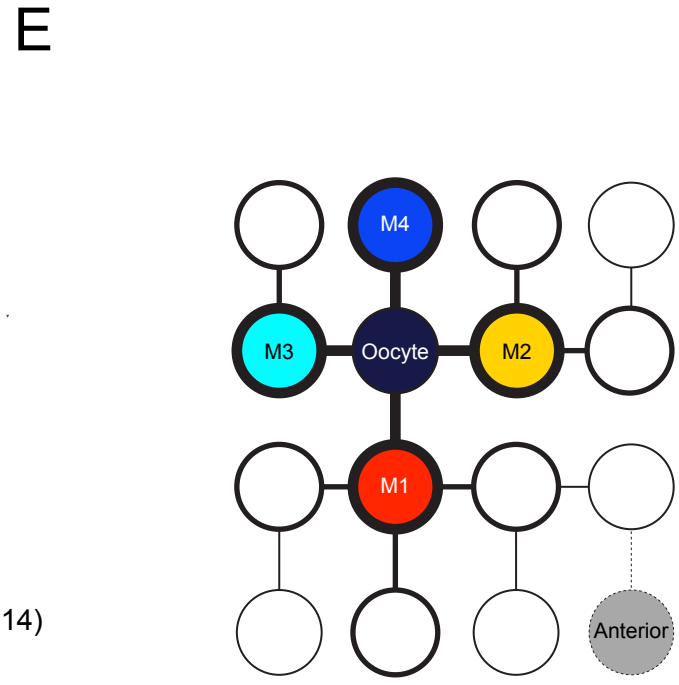
E
M4
M3
Oocyte
M2
M1
Anterior

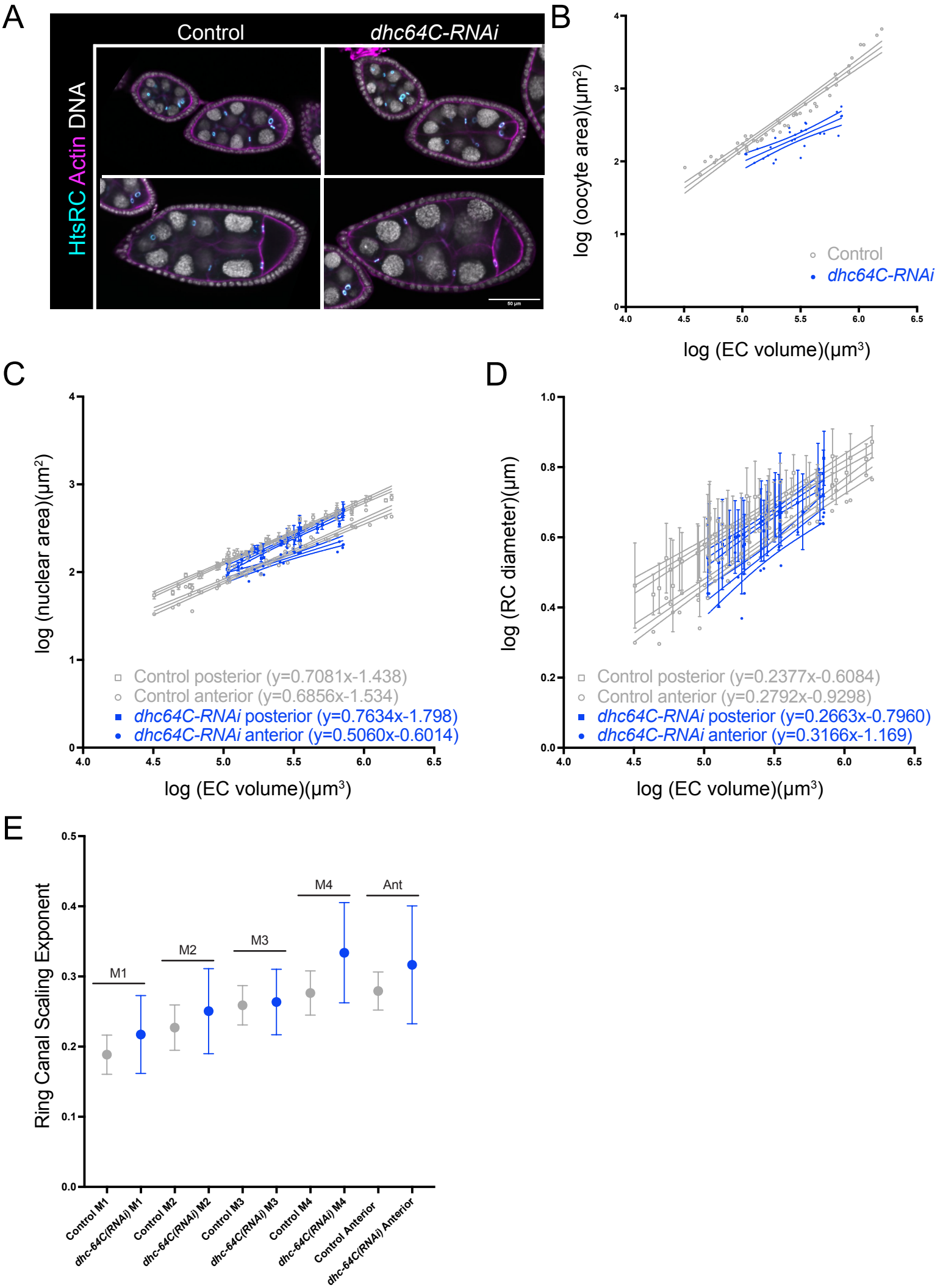
A
Control
dhc64C-RNAi
HtsRC Actin DNA
50 µm
B
log (oocyte area)(µm²)
log (EC volume)(µm³)
Control
dhc64C-RNAi
C
log (nuclear area)(µm²)
log (EC volume)(µm³)
Control posterior (y=0.7081x-1.438)
Control anterior (y=0.6856x-1.534)
dhc64C-RNAi posterior (y=0.7634x-1.798)
dhc64C-RNAi anterior (y=0.5060x-0.6014)
D
log (RC diameter)(µm)
log (EC volume)(µm³)
Control posterior (y=0.2377x-0.6084)
Control anterior (y=0.2792x-0.9298)
dhc64C-RNAi posterior (y=0.2663x-0.7960)
dhc64C-RNAi anterior (y=0.3166x-1.169)
E
Ring Canal Scaling Exponent
M1
M2
M3
M4
Ant
Control M1
dhc-64C(RNAi) M1
Control M2
dhc-64C(RNAi) M2
Control M3
dhc-64C(RNAi) M3
Control M4
dhc-64C(RNAi) M4
Control Anterior
dhc-64C(RNAi) Anterior

Figure 3

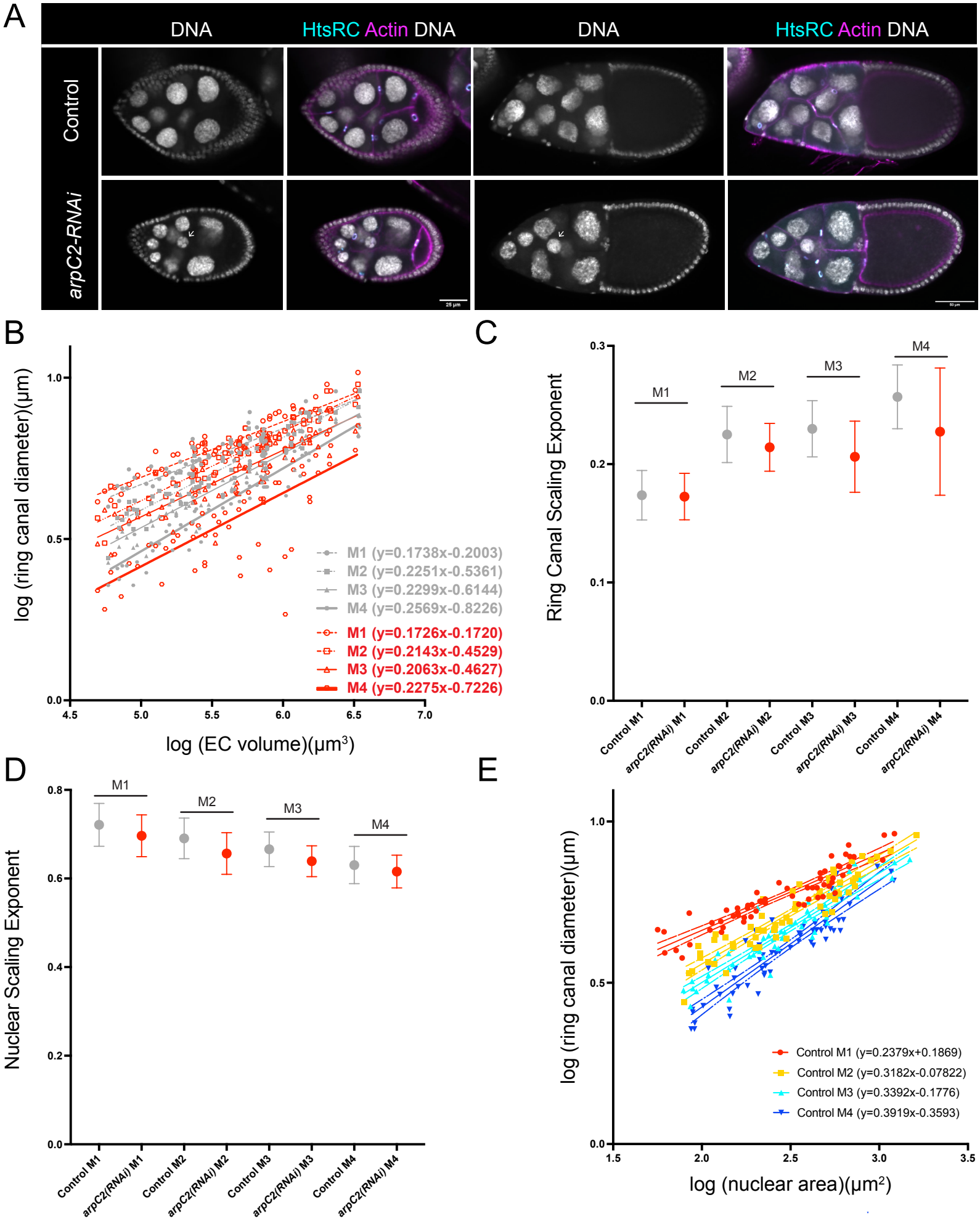
A
DNA
HtsRC Actin DNA
DNA
HtsRC Actin DNA
Control
arpC2-RNAi
B
log (ring canal diameter)(µm)
log (EC volume)(µm³)
M1 (y=0.1738x-0.2003)
M2 (y=0.2251x-0.5361)
M3 (y=0.2299x-0.6144)
M4 (y=0.2569x-0.8226)
M1 (y=0.1726x-0.1720)
M2 (y=0.2143x-0.4529)
M3 (y=0.2063x-0.4627)
M4 (y=0.2275x-0.7226)
C
Ring Canal Scaling Exponent
M1
M2
M3
M4
Control M1
arpC2(RNAi) M1
Control M2
arpC2(RNAi) M2
Control M3
arpC2(RNAi) M3
Control M4
arpC2(RNAi) M4
D
Nuclear Scaling Exponent
M1
M2
M3
M4
Control M1
arpC2(RNAi) M1
Control M2
arpC2(RNAi) M2
Control M3
arpC2(RNAi) M3
Control M4
arpC2(RNAi) M4
E
log (ring canal diameter)(µm)
log (nuclear area)(µm²)
Control M1 (y=0.2379x+0.1869)
Control M2 (y=0.3182x-0.07822)
Control M3 (y=0.3392x-0.1776)
Control M4 (y=0.3919x-0.3593)

Figure 4

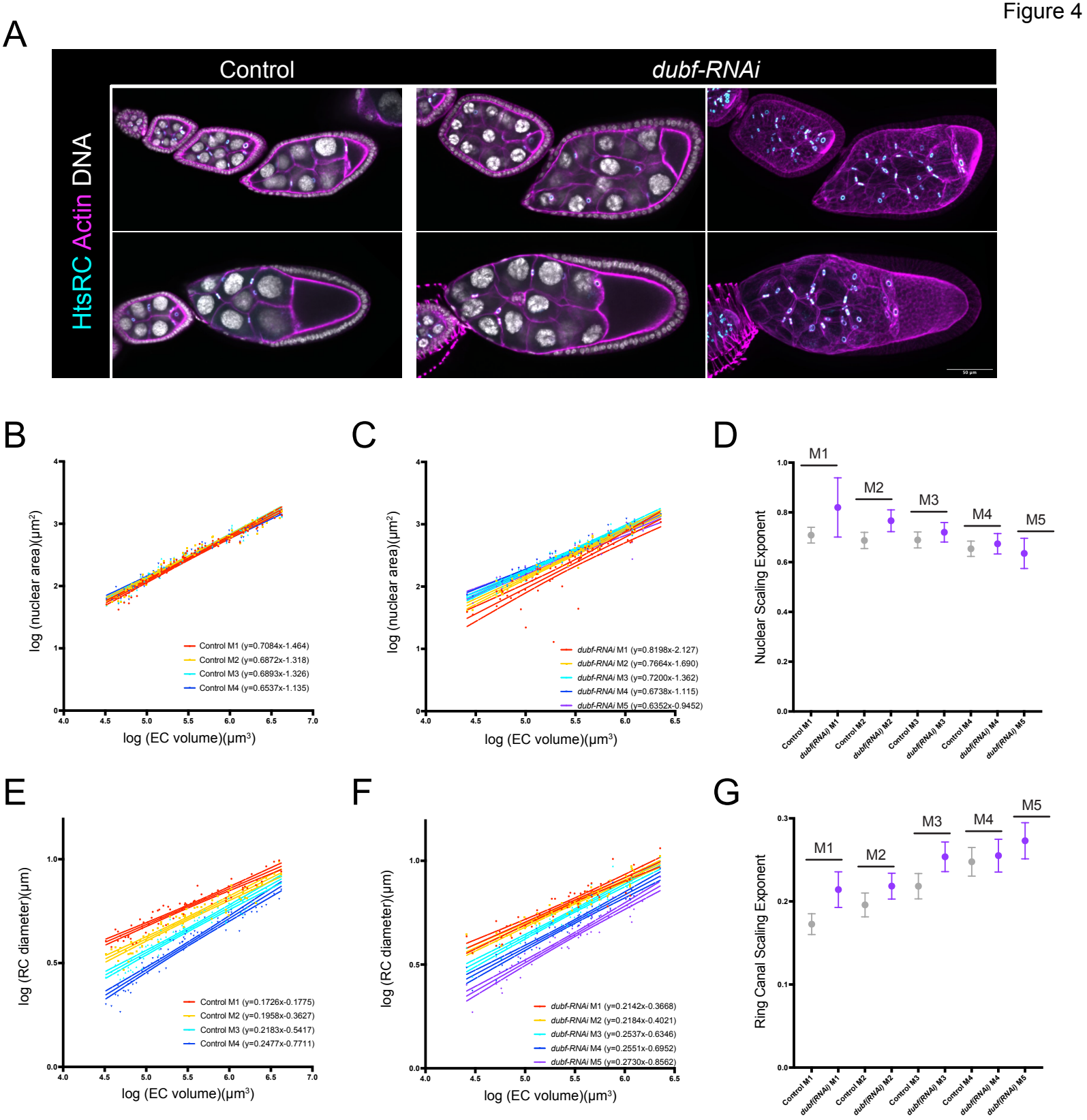
A
Control
dubf-RNAi
HtsRC Actin DNA
B
log (nuclear area)(μm²)
log (EC volume)(μm³)
Control M1 (y=0.7084x-1.464)
Control M2 (y=0.6872x-1.318)
Control M3 (y=0.6893x-1.326)
Control M4 (y=0.6537x-1.135)
C
log (nuclear area)(μm²)
log (EC volume)(μm³)
dubf-RNAi M1 (y=0.8198x-2.127)
dubf-RNAi M2 (y=0.7664x-1.690)
dubf-RNAi M3 (y=0.7200x-1.362)
dubf-RNAi M4 (y=0.6738x-1.115)
dubf-RNAi M5 (y=0.6352x-0.9452)
D
Nuclear Scaling Exponent
M1
M2
M3
M4
M5
Control M1
dubf(RNAi) M1
Control M2
dubf(RNAi) M2
Control M3
dubf(RNAi) M3
Control M4
dubf(RNAi) M4
dubf(RNAi) M5
E
log (RC diameter)(μm)
log (EC volume)(μm³)
Control M1 (y=0.1726x-0.1775)
Control M2 (y=0.1958x-0.3627)
Control M3 (y=0.2183x-0.5417)
Control M4 (y=0.2477x-0.7711)
F
log (RC diameter)(μm)
log (EC volume)(μm³)
dubf-RNAi M1 (y=0.2142x-0.3668)
dubf-RNAi M2 (y=0.2184x-0.4021)
dubf-RNAi M3 (y=0.2537x-0.6346)
dubf-RNAi M4 (y=0.2551x-0.6952)
dubf-RNAi M5 (y=0.2730x-0.8562)
G
Ring Canal Scaling Exponent
M1
M2
M3
M4
M5
Control M1
dubf(RNAi) M1
Control M2
dubf(RNAi) M2
Control M3
dubf(RNAi) M3
Control M4
dubf(RNAi) M4
dubf(RNAi) M5

Figure 5

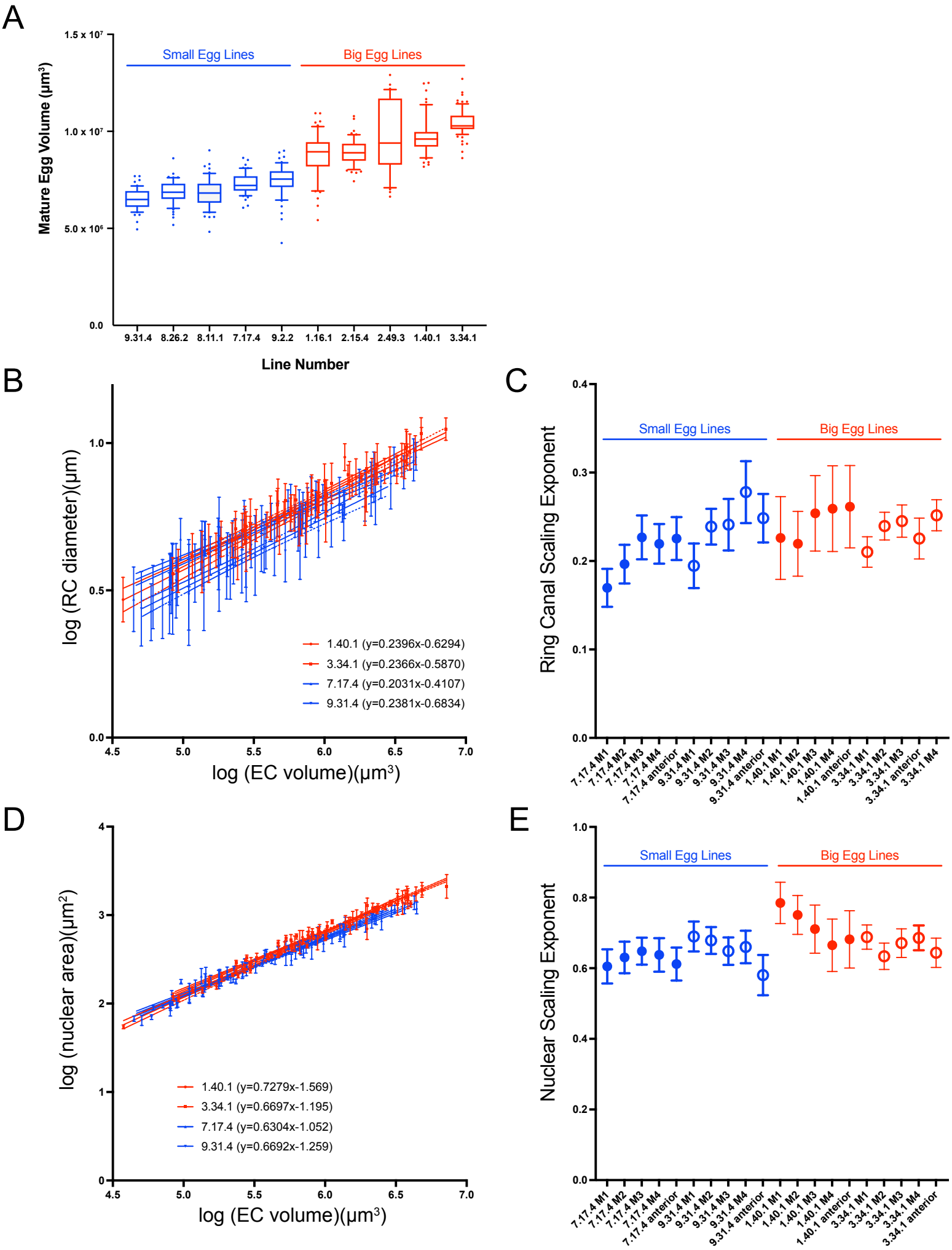
A
Small Egg Lines
Big Egg Lines
Mature Egg Volume (µm³)
1.5 x 10⁷
1.0 x 10⁷
5.0 x 10⁶
0.0
9.31.4 8.26.2 8.11.1 7.17.4 9.2.2 1.16.1 2.15.4 2.49.3 1.40.1 3.34.1
Line Number
B
log (RC diameter)(µm)
log (EC volume)(µm³)
1.40.1 (y=0.2396x-0.6294)
3.34.1 (y=0.2366x-0.5870)
7.17.4 (y=0.2031x-0.4107)
9.31.4 (y=0.2381x-0.6834)
C
Ring Canal Scaling Exponent
Small Egg Lines
Big Egg Lines
7.17.4 M1 7.17.4 M2 7.17.4 M3 7.17.4 M4 7.17.4 anterior 9.31.4 M1 9.31.4 M2 9.31.4 M3 9.31.4 M4 9.31.4 anterior 1.40.1 M1 1.40.1 M2 1.40.1 M3 1.40.1 M4 1.40.1 anterior 3.34.1 M1 3.34.1 M2 3.34.1 M3 3.34.1 anterior 3.34.1 M4
D
log (nuclear area)(µm²)
log (EC volume)(µm³)
1.40.1 (y=0.7279x-1.569)
3.34.1 (y=0.6697x-1.195)
7.17.4 (y=0.6304x-1.052)
9.31.4 (y=0.6692x-1.259)
E
Nuclear Scaling Exponent
Small Egg Lines
Big Egg Lines
7.17.4 M1 7.17.4 M2 7.17.4 M3 7.17.4 M4 7.17.4 anterior 9.31.4 M1 9.31.4 M2 9.31.4 M3 9.31.4 M4 9.31.4 anterior 1.40.1 M1 1.40.1 M2 1.40.1 M3 1.40.1 M4 1.40.1 anterior 3.34.1 M1 3.34.1 M2 3.34.1 M3 3.34.1 M4 3.34.1 anterior

Figure S1

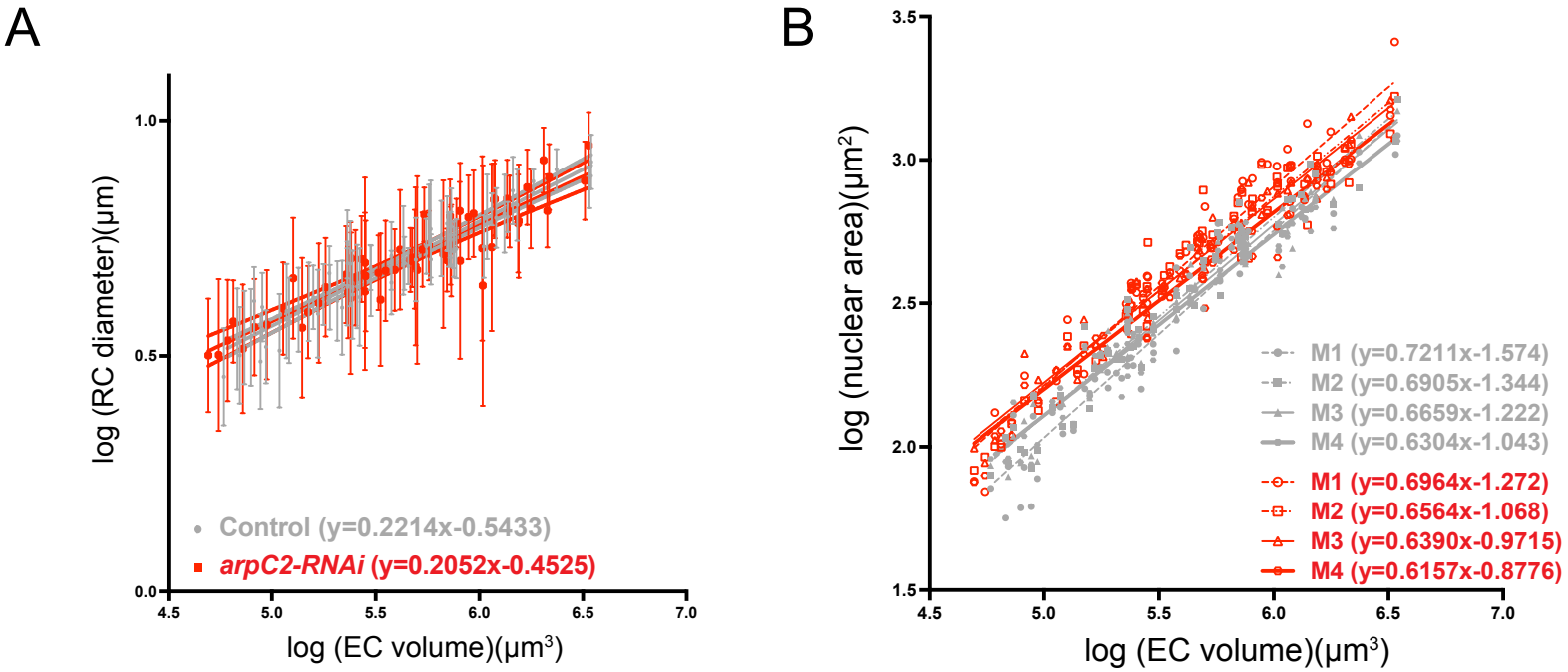
A
log (RC diameter)(μm)
1.0
0.5
0.0
4.5
5.0
5.5
6.0
6.5
7.0
log (EC volume)(μm³)
Control (y=0.2214x-0.5433)
arpC2-RNAi (y=0.2052x-0.4525)
B
log (nuclear area)(μm²)
3.5
3.0
2.5
2.0
1.5
4.5
5.0
5.5
6.0
6.5
7.0
log (EC volume)(μm³)
M1 (y=0.7211x-1.574)
M2 (y=0.6905x-1.344)
M3 (y=0.6659x-1.222)
M4 (y=0.6304x-1.043)
M1 (y=0.6964x-1.272)
M2 (y=0.6564x-1.068)
M3 (y=0.6390x-0.9715)
M4 (y=0.6157x-0.8776)

Figure S2

A

Nuclear Scaling

	Slope	Intercept
1.40.1 M1	0.7849	-1.864
1.40.1 M2	0.7508	-1.685
1.40.1 M3	0.7107	-1.474
1.40.1 M4	0.665	-1.254
1.40.1 Anterior	0.6817	-1.554
3.34.1 M1	0.6881	-1.279
3.34.1 M2	0.6339	-0.9792
3.34.1 M3	0.671	-1.208
3.34.1 M4	0.6859	-1.314
3.34.1 Anterior	0.6437	-1.314
7.17.4 M1	0.6051	-0.8769
7.17.4 M2	0.6305	-1.037
7.17.4 M3	0.6483	-1.17
7.17.4 M4	0.6377	-1.123
7.17.4 Anterior	0.6119	-1.156
9.31.4 M1	0.6898	-1.342
9.31.4 M2	0.6785	-1.286
9.31.4 M3	0.6484	-1.153
9.31.4 M4	0.6602	-1.257
9.31.4 Anterior	0.5805	-0.9742

Ring Canal Scaling

	Slope	Intercept
1.40.1 M1	0.226	-0.4801
1.40.1 M2	0.2195	-0.492
1.40.1 M3	0.2539	-0.7339
1.40.1 M4	0.2592	-0.8118
1.40.1 Anterior	0.2614	-0.8459
3.34.1 M1	0.2102	-0.3782
3.34.1 M2	0.2395	-0.5769
3.34.1 M3	0.2451	-0.6539
3.34.1 M4	0.2517	-0.739
3.34.1 Anterior	0.2254	-0.619
7.17.4 M1	0.1697	-0.1555
7.17.4 M2	0.1965	-0.3532
7.17.4 M3	0.2267	-0.5642
7.17.4 M4	0.2194	-0.5698
7.17.4 Anterior	0.2254	-0.5934
9.31.4 M1	0.1946	-0.3516
9.31.4 M2	0.2388	-0.6368
9.31.4 M3	0.2411	-0.7217
9.31.4 M4	0.2779	-1.023
9.31.4 Anterior	0.2484	-0.822

B

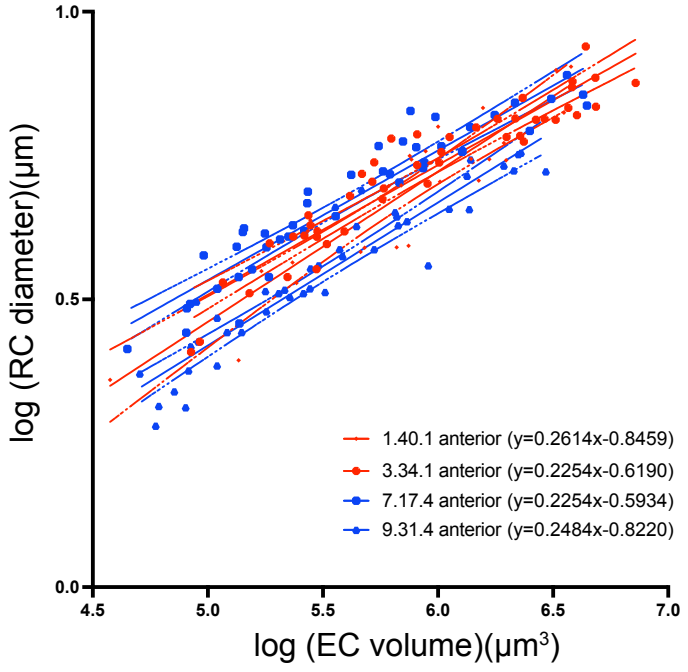
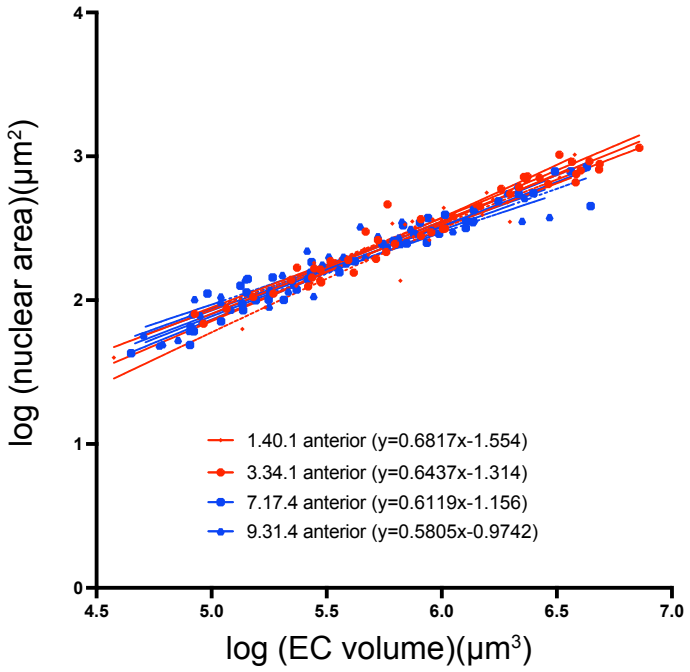
C